*J. Res. Inst. Catalysis, Hokkaido Univ., Vol. 25, No. 2, pp. 45 to 62 (1977)*

# ELECTROREDUCTION OF ACETONE ON PLATINUM IN SULFURIC ACID SOLUTION AND CATALYTIC ACTION OF PLATINUM AND MERCURY ELECTRODES

By

Hideaki KITA*, Kenji SAITO* and Akiko KATAYAMA**

(Received May 11, 1977)

**Abstract**

Electroreduction of acetone was conducted on smooth and platinized platinum electrodes in aqueous sulfuric acid solution. Acetone is reduced with a much slower rate, *ca.* a thousandth, than ethylene on a platinum electrode. Propane is produced with a selectivity of >90% on the platinized platinum electrode. Mechanistic study leads to the conclusion that (i) hydrogen atom and acetone adsorb on different facets (or different kind of sites), (ii) in the TAFEL line region, the combination of the adsorbed hydrogen and acetone at the boundary between the two facets is rate-controlling, and (iii) the limiting current is due to the surface diffusion of the adsorbed acetone to the boundary (or the change in the ad-sorption state).

Difference of the reaction rate between the smooth and the platinized platinum electrodes is mainly attributed to that of the surface area. Hydrogen electrode reaction on a platinum electrode is discussed in term of the diffusion of the evolved hydrogen into the solution.

## Introduction

ANTROPOV[1] concluded that metals of high hydrogen overvoltage are active in the reduction of polar bonds such as >C=O and metals of low hydrogen overvoltage are active in the reduction of non-polar bonds such as >C=C<. One of the present authors[2] compared catalytic actions of metal electrodes with respect to the hydrogen electrode reaction and the electroreduction of organic compounds and concluded that transition metals including gold, silver and copper (named *d*-metals) and metals after IIB in the periodic table (named *sp*-metals) show essentially different catalytic actions in harmony with ANTROPOV's conclusion. In addition, he pointed out that steric selectivity is also different between the *d*- and *sp*-metals ; *cis* addition

*) Dept. of Chem., Faculty of Science, Hokkaido University, Sapporo 060, Japan
**) Res. Inst. for Catalysis, Hokkaido University, Sapporo 060, Japan

of hydrogen selectively takes place on *d*-metals, whereas *trans* addition on *sp*-metals, respectively.[2]

This study was carried out to confirm the above difference of the catalytic action by performing the electroreduction of acetone (>C=O) on platinum (*d*-metal) electrode in acid solution. Results are compared with those on the electroreductions of ethylene (>C=C<) on platinum and of ethylene and acetone on mercury (*sp*-metal). Kinetics of the acetone electroreduction is discussed in detail.

## Experimental

*Cell*: Cell used was of a type of three compartments. The cell was cleaned with chromic acid mixture or a mixture of concentrated sulfuric acid and nitric acid, washed with triply distilled water, and then finally treated by the water vapor steaming for a few hours.

*Material*: Platinum electrode (purity>99.9%) was a smooth or platinized platinum wire. Mercury which was used in a supplementary experiment was purified by repeating distillation four times under vacuum, and used in the form of dropping or pool electrode. Hydrogen and helium were purified by commercially available purifiers (the membrane type for $H_2$ and the getter type for He). Ethylene was purified by repeating distillation three times under vacuum. All solutions were prepared by using chemical reagents of special grade.

*Measurement*: The TAFEL plot was observed by the galvanostatic or potentiostatic methods. Reference electrode was the reversible hydrogen electrode in the same solution as in the test electrode compartment but without acetone or ethylene.

The macroscale electrolysis was carried out by the potentiostatic method on platinized platinum net (apparent area, 6 $cm^2$) or mercury pool electrode (area, 14 $cm^2$).

Ethylene reduction was conducted by circulating the reactant gas through the cell with a flow rate of ca. 100 m*l*/min.[3] The gas was occasionally sampled for analysis.

Analysis of products was carried out by a gas chromatography (FID, PEG 400, 100°C for $i$-$C_3H_7OH$; TCD, silica gel, 50°C for $C_2H_6$, $C_2H_4$, VZ-7 for $C_3H_8$).

## Results

### 1. Open circuit potential.

Open circuit potential provides a useful information for the analysis of

the rates of two or more reactions occurring on the electrode.

Fig. 1 shows the open circuit potentials on smooth and platinized platinum electrodes (denoted as smooth-Pt and pt-Pt) measured in $H_2$-saturated 6 N-$H_2SO_4$ solution containing a different amount of acetone. The open circuit potential on smooth-Pt is almost constant and equal to the value of the reversible hydrogen electrode when the acetone concentration is smaller than $10^{-1}$M. At 1M acetone, it slightly shifts in the positive direction, *i. e.*, *ca.* +10 mV (RHE).

On the contrary, the open circuit potential of pt-Pt becomes *ca.* 100 mV (RHE) when the acetone concentration exceeds $10^{-2}$M.

The open circuit potential in ethylene saturated solution has been described earlier in detail.[3)]

**2. Time variation of current.**

Current at a constant polarization shows the time variation under the presence of acetone as shown in Fig. 2.

Ratio of $i_t/i_{t=1\,\mathrm{min}}$ decreases linearly with log $t$ at each potential. Its slope becomes identical after 4~10 min; $\mathrm{d}(i/i_{t=1\,\mathrm{min}})/\mathrm{d}\log t=0.32$ being independent of potential. Thus, the TAFEL relation is examined by using the value at 20 min at which the variation of the current, $\mathrm{d}(i_{t=20\,\mathrm{min}}/i_{t=1\,\mathrm{min}})/\mathrm{d}t$, is smaller than 1%.

Time variation of current was absent in the blank solution at all potentials studied.

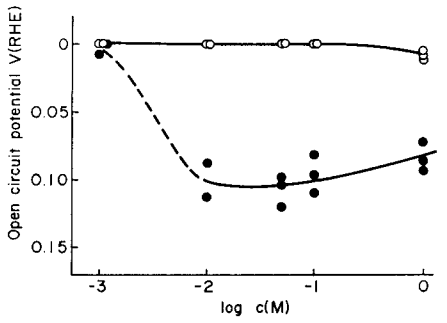


**Fig. 1.** Dependence of the open circuit potential on the acetone concentration on a smooth (○) and platinized (●) platinum electrodes in $H_2$-saturated 6N $H_2SO_4$.

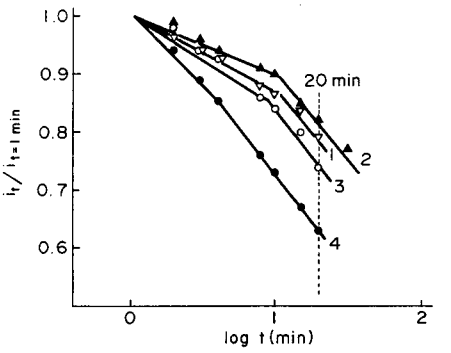


**Fig. 2.** Time variation of current on smooth (1) and platinized (2~4) platinum electrodes in He-saturated 6N $H_2SO_4$. Acetone concentration and potential (RHE) are: 1, $10^{-2}$M, +10 mV; 2, $10^{-3}$M, +10 mV; 3, $10^{-1}$ M, +10 mV; 4, $10^{-1}$M, +100 mV.

### 3. The TAFEL relation.

*3-1). $(CH_3)_2CO$ electroreduction on Pt.*

Figs. 3 a and 3 b show the TAFEL relation of the electroreduction of acetone on smooth-Pt and pt-Pt in He-saturated 6N-$H_2SO_4$ with various acetone concentrations. When 1N-$H_2SO_4$ was used, the reduction current of acetone was hardly detected on smooth-Pt and hence more concentrated solution was used.

TAFEL lines of the hydrogen electrode reaction coincide each other on both smooth-Pt and pt-Pt, irrespective of the large difference in their real surface area. They are expressed as follows,

$$\eta(\mathrm{V}) = -0.09 - 0.03 \log i \quad (\mathrm{A/geom.\ cm^2}), \qquad (1)$$

where $\eta$ represents the electrode potential referred to the reversible hydrogen electrode and the current density is expressed for their geometrical surface area.

When acetone is introduced into the solution, an increase of cathodic current was observed in a potential range more positive than RHE, indicating the electroreduction of acetone. The current increase appeared much more clearly on pt-Pt (Fig. 3 b).

The TAFEL line exists at low current densities, being independent of the acetone concentration at $>10^{-2}$M (Fig. 3 b), and is expressed by the following equation on pt-Pt.

$$\eta(\mathrm{V}) = 0.03 - 0.03 \log i \quad (\mathrm{A/geom.\ cm^2}). \qquad (2)$$

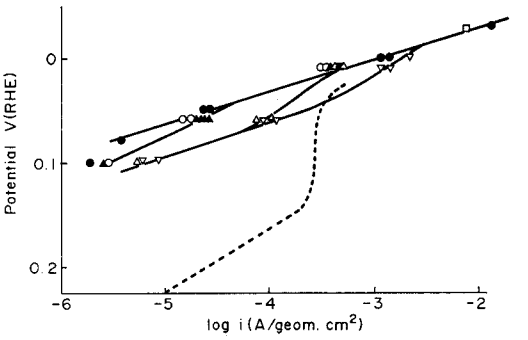


**Fig. 3 a.** TAFEL plots of the acetone electroreduction on a smooth-Pt in He-saturated 6N $H_2SO_4$ with the acetone concentration of: ●, 0; ○, $10^{-3}$M; ▲, $10^{-2}$M; △, $10^{-1}$M; ▽, 1 M. Dotted curve is for the electroreduction of ethylene dissolved in 1 N $H_2SO_4$ at 1 atm.

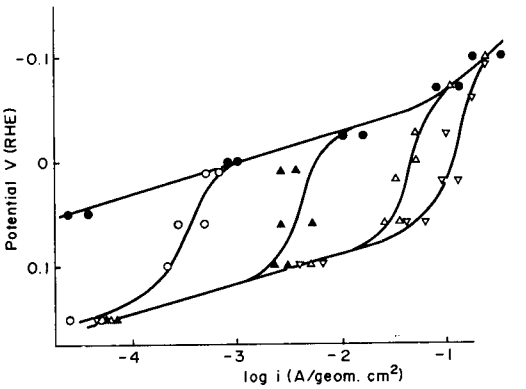


**Fig. 3 b.** TAFEL plots of the acetone electroreduction on a platinized-Pt in He-saturated 6M $H_2SO_4$ with the acetone concentration of: ●, 0; ○, $10^{-3}$M; ▲, $10^{-2}$M; △, $10^{-1}$M; ▽, 1M.

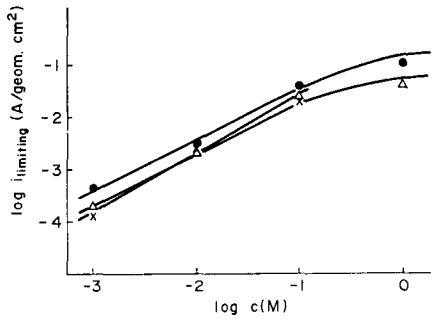


**Fig. 4.** Limiting current on a platinized-Pt as a function of the acetone concentration at various acid concentrations (He-saturated). ●, 6N $H_2SO_4$; ×, 1N $H_2SO_4$; △, 0.3N $H_2SO_4$

TABLE 1. The pH dependence of the acetone reduction current in the region of the TAFEL line

| Conc. of acetone (M) | log $i$ (A/cm²) at 0.10 V (NHE) | | $\Delta \log i / \Delta \log a_{H^+}$ |
|---|---|---|---|
| | 6N $H_2SO_4$ | 1N $H_2SO_4$ | |
| 1 | −2.52 | −4.66 | 2.38 |
| | −2.74 | | 2.11 |
| $10^{-1}$ | −2.64 | −4.55 | 2.18 |
| | −2.77 | | 2.02 |
| $10^{-2}$ | −2.82 | −4.60 | 2.03 |
| | −2.92 | | 1.91 |

Mean value 2.11

With the increase of the cathodic polarization, the current approaches to a limiting value and then finally follows the relation observed for the hydrogen evolution reaction. The limiting current increases with the increase of the acetone concentration as shown in Fig. 4. The limiting current, represented by the inflection point of the S-shape TAFEL relation, is proportional to the acetone concentration up to 0.1 M (slope of $\log i$-$\log c$ plot = 0.95). Solution pH does not affect the limiting current.

Decrease of the acid concentration, however, causes a shift of the TAFEL line of Eq. (2) in the negative direction of $\eta$. The reaction order with respect to $H^+$ is estimated as 2 in the TAFEL region (Table 1.)

On smooth-Pt, the increase of current by the introduction of acetone is not large enough to be analysed, *ca.* one thousandth smaller than that on pt-Pt in the region of the TAFEL line. Such a difference will be mainly due to the difference in the roughness factor, suggesting that the surface reaction controls the reaction rate.

*3-2). $C_2H_4$ electroreduction on Hg.*

Fig. 5 shows TAFEL relations under the presence of ethylene on mercury electrode in He-saturated 1N $H_2SO_4$ solution (curve 1) and 1N NaOH solution (curve 2), respectively.

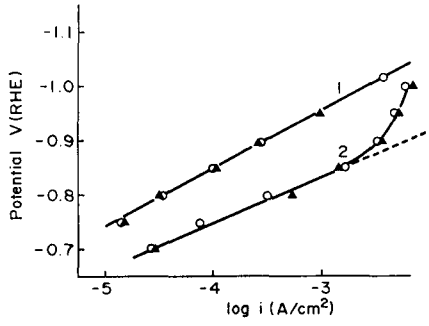


**Fig. 5.** TAFEL plots on mercury in He-saturated 1N $H_2SO_4$ (1) and 1N NaOH (2) solutions under the absence (○) or presence (▲) of ethylene (1 atm).

TAFEL lines (slope; 105 mV in 1N-$H_2SO_4$ and 80 mV in 1N-NaOH) reproduce the reported ones on the hydrogen electrode reaction[4~7] and are not affected by the introduction of ethylene within the experimental error, indicating no reduction of ethylene on mercury.

**4. Potential sweep.**

*4-1). Roughness factor.*

Roughness factor was estimated from the amount of adsorbed hydrogen in the hydrogen region of I-V curves by using the value of 210 $\mu$C per true unit surface area. Sweep rates were 14.4 V/s*) on smooth-Pt and 10 mV/s, 30 mV/s, 1 V/s and 36 V/s on pt-Pt, respectively.

For the sake of the precise estimation of the amount of adsorbed hydrogen, we first examined if the current in the double layer region ($I_D$) is given as the sum of the ionization current of the dissolved hydrogen molecule ($I_D^L$) and the charging current of the double laryer ($I_{D1}$).

$I_D^L$ in 6N $H_2SO_4$ solution was estimated by the constant polarization of the electrode in the double layer region. Steady current in this case does not contain $I_{D1}$. Table 2 shows $I_D^L$ at 0.5 V in the solution saturated with hydrogen gas of 1 atm. This value was almost constant at potentials >0.1 V on both smooth-Pt and pt-Pt.

$I_{D1}$ was estimated from the I-V curves taken in a potential range from 0.4 to 1.8 V in the He saturated solution. In this case, the current does not contain $I_D^L$. The electrode surface will be free from the adsorbed hydrogen,

TABLE 2. Analysis of the current at 0.5 V (double layer region) and the amount of the adsorbed hydrogen

| | sweep rate (V/s) | $I_{D1}$ (mA/geom. cm$^2$) | $I_D$ (mA/geom. cm$^2$) | $I_{D1}+I_D^L$ (mA/geom. cm$^2$) | $Q_H$ (C/geom. cm$^2$) |
|---|---|---|---|---|---|
| smooth-Pt | 14.4 | 2.55 | 4.71 | 4.73 | $0.6\times10^{-3}$ |
| | Constant polarization at 0.5 V, $I_D^L$=2.18 mA/geom. cm$^2$ | | | | |
| pt-Pt | 0.010 | 0.13 | 3.38 | 2.68 | $9.3\times10^{-2}$ |
| | 0.030 | 0.29 | 4.20 | 2.84 | $7.6\times10^{-2}$ |
| | 1 | 5.86 | 8.82 | 8.41 | $3.7\times10^{-2}$ |
| | 3.6 | 21.5 | 24.5 | 24.05 | $3.9\times10^{-2}$ |
| | Constant polarization at 0.5 V, $I_D^L$=2.55 mA/geom. cm$^2$ | | | | |

*) As reported that the amount of adsorbed hydrogen is constant at sweep rate within 20 V/s on smooth-Pt[8], a sweep rate of 14.4 V/s was used.

since the electrode is polarized in the positive direction more than 0.4 V. Currents at 0.5 V are shown as $I_{D1}$ in Table 2.

Another I-V curve was taken in a potential range from 0 to 1.8 V (RHE) in the solution saturated with 1 atm hydrogen. Values of current at 0.5 V are shown as $I_D$ in Table 2.

As seen from Table 2, $I_D$ on smooth-Pt shows a good agreement with the sum of $I_D^L$ and $I_{D1}$. Therefore, the amount of adsorbed hydrogen is estimated by subtracting $I_D(=I_D^L+I_{D1})$ from the observed current. Roughness factor thus obtained is 2.88.

On the other hand, $I_D$ on pt-Pt does not coincide with the sum of $I_D^L+I_{D1}$ at lower sweep rate.

The amount of adsorbed hydrogen, $Q_H$, was estimated by subtracting the sum of $I_D^L$ and $I_{D1}$ from the observed current in a potential range from 0 to 0.8 V. Roughness factor thus obtained on pt-Pt in $H_2$-saturated 6N $H_2SO_4$ is a function of the sweep rate as shown in Fig. 6 (curve 1). The roughness factor decreases with the increase of sweep rate and approaches a constant value when sweep rate exceeds 1 V/s. At the sweep rate larger than 1 V/s, $I_D$ is in agreement with the sum of $I_D^L+I_{D1}$ as seen from the Table 2. The same result as Fig. 6 was obtained from the first I-V curves taken immediately after the anodic activation.

*4-2). Effect of cavities in the pt-Pt.*

The sweep rate dependence of the roughness factor of pt-Pt may be caused by the reason that the adsorbed hydrogen or/and the hydrogen molecule in small cavities in the deposited layer of pt-Pt slowly responds to the potential change. If so, $I_{D1}$ which does not contain the ionization of hydrogen is expected to be proportional to the sweep rate, which was not

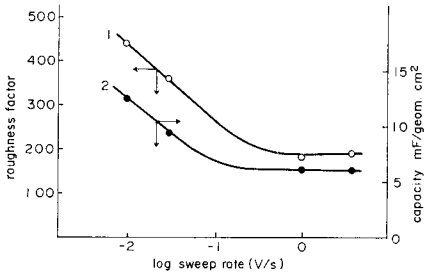


**Fig. 6.** Dependence of the roughness factor (○) and capacity (●) on the sweep rate at platinized-Pt in $H_2$-saturated 6N $H_2SO_4$.

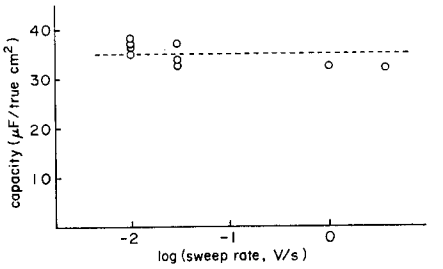


**Fig. 7.** Capacity for the true unit area of platinized-Pt estimated at different sweep rate ($H_2$-saturated 6N $H_2SO_4$).

the case, as seen from Table 2.

The double layer capacity $C_D$, calculated by the equation $C_D = I_{D1}/S$ where $S$ is the sweep rate, is shown in Fig. 6 (curve 2). When $C_D$ thus calculated is further devided by the roughness factor, almost a constant value is obtained as shown in Fig. 7. In this calculation, the curve 1 in Fig. 6 was used for the roughness factor at each sweep rate. The constant value of $30 \sim 40\ \mu F/cm^2$ coincides with the reported ones.[9,10] Absence of the sweep rate dependence denies the possibility that any dissolved hydrogen molecules in cavities of pt-Pt or the adsorbed hydrogen on cavity surface ionize more at slower sweep rates and contribute to the apparent increase of the roughness factor. The present results may indicate that the potential distribution in the cavities is set up in an inductive way.

The true roughness factor should be obtained by the extrapolation of the roughness factor *vs.* the sweep rate curve to the limiting case of $S=0$. The extrapolation is practically difficult because a proper functional form was not found between the roughness factor and the sweep rate. Hence, we conventionally assume a value of 400 for the roughness factor. This assumption does not introduce any ambiguity in discussion of the relative quantities of the present results.

**5. Macroscale electrolysis.**

Results of the macroscale electrolysis on pt-Pt under the presence of acetone in He-saturated 6N $H_2SO_4$ are shown in Table 3. As seen from Table 3, the main product is propane. Current efficiency for the acetone electroreduction is $81 \sim 84\%$ at $0.06 \sim 0.1$ V on pt-Pt, whereas according to our supplementary experiments *ca.* 27% on smooth-Pt. The rest is used for the hydrogen evolution.

TABLE 3. Macroscale electrolysis on pt-Pt under the presence of acetone

| Electrode | Potential (V *vs.* RHE) | Acetone (M) | Product | | Selectivity | | Current efficiency | |
|---|---|---|---|---|---|---|---|---|
| | | | isopropanol (M) | propane (M) | isopropanol | propane | isopropanol | propane |
| pt-Pt | +0.06 | $10^{-1}$ | (0.5~0.6) $\times 10^{-5}$ | 1.5 $\times 10^{-4}$ | (3.4~4.2) % | (96~97) % | (1.5~1.8) % | 82 % |
| | | | | | | | 84% | |
| pt-Pt | +0.1 | $10^{-1}$ | (0.4~0.5) $\times 10^{-5}$ | 8.4 $\times 10^{-5}$ | (4.5~6.1) % | (94~96) % | (1.9~2.5) % | 79 % |
| | | | | | | | 81% | |

TABLE 4. Macroscale electrolysis on mercury electrode under the presence of ethylene

| Electrolyte | Potential (V *vs.* RHE) | Ethylene (cmHg) | Electricity passed (Coul.) | Product |
|---|---|---|---|---|
| 1N $H_2SO_4$ | −0.90 | 12.3 | 470 | No ethane was detected |
| 1N $H_2SO_4$ | −1.05 | 13.1 | 690 | |
| 1N NaOH | −1.02 | 6.0 | 260 | |
| 1N NaOH | −0.96 | 2.8 | 270 | |

Macroscale electrolysis on mercury was conducted under the presence of ethylene. Experimental conditions and results are shown in Table 4. No ethane was detected by a gaschromatography. It is to be noted here that acetone is well reduced on the mercury electrode,[7] giving isopropanol as a main product with a current efficiency of 71% at −1.2 V (NHE) in 1N $H_2SO_4$.

## Discussion

### 1. Electrocatalysis by electrode metals.

Electroreduction rates of acetone and ethylene are compared on platinum and mercury electrodes in Table 5. Each figures are reproduced from Figs. 3 a, 5 and Ref. (7). On smooth-Pt, ethylene is reduced with a rate $10^3$ times larger than that of acetone at a potential of 0.15 V (RHE). On mercury, however, acetone is easily reduced with a large rate[7] but no reduction of ethylene is observed even at a high cathodic polarization. These facts recomfirm the proposal of ANTROPOV[1] and one of the present authors.[2]

Electroreduction of acetone is apparently accelerated to a large extent on pt-Pt. When we take into account the roughness factor, the reaction rate is reduced at least by two orders of magnitude and will become comparable with the rate on smooth-Pt. Any possible effect of Pb which might be occluded during the platinization was discarded by the experiment on the electrode platinized under the absence of $Pb(OAc)_2$.

### 2. Product of the acetone electroreduction.

It has been reported that the products in the acetone electroreduction on pt-Pt are isopropanol and propane,[11] depending on the electrode potential and the history of the electrode. With an electrode which has been freshly

TABLE 5. Electroreduction rates of acetone and ethylene

| electrode | solution | potential | Current (A/cm²) | |
|---|---|---|---|---|
| | | | $C_2H_4$ (1 atm) | $(CH_3)_2CO$ (1M) |
| smooth-Pt | 6N $H_2SO_4$ | 0.15 V (RHE) | $2\times10^{-4}$ | $2\times10^{-7}$ |
| Hg | 1N $H_2SO_4$ | −1.1 V (NHE) | 0 | $4.0\times10^{-1}$[7] |

activated by an anodic treatment, propane is the only product. If, however, the electrode is made more negative than the potential of RHE, the rate of isopropanol formation increases during the first few hours, with a simultaneous decrease of the rate of formation of propane. After about 15～20 h, hydrogen evolution is the only remaining electrode process.

They had concluded[11] that an interstitial hydrogen is involved in the reaction path leading to isopropanol, whereas surface hydrogen plays a more important role in the reaction path leading to propane.

Standard potentials of the following reactions

$$CH_3COCH_3+2H^++2e^-\longrightarrow CH_3CH(OH)CH_3 \qquad (3)$$

$$CH_3COCH_3+4H^++4e^-\longrightarrow CH_3CH_2CH_3+H_2O \qquad (4)$$

are calculated from thermodynamical data[12] as +136 mV (NHE) for Eq. (3) and +252 mV (NHE) for Eq. (4), respectively. These numerical values indicate that the propane formation accompanies a greater chemical affinity. Present results obtained on the freshly activated electrode (Table 3) are in agreement with the thermodynamical expectation and reproduce the reported one.[11]

**3. Limiting current at the acetone electroreduction.**

The limiting current on platinum electrodes was not affected by He bubbling. Nature of the limiting current was examined as follows.

i) The limiting diffusion rate of acetone was estimated approximately as 4.94 A/cm² at 1 M by the equation of $I=nFDc/\delta$, where $n$ is the number of electron concerned with the reaction, $(CH_3)_2CO+4H^++4e^-\rightarrow CH_3CH_2CH_3$, $F$ the Faraday, $D$ the diffusion constant, $1.28\times10^{-5}$ cm²/sec,[13] $\delta$ the diffusion layer thickness, $10^{-3}$ cm, and $c$ the acetone concentration, respectively. The limiting diffusion rate is about fifty times larger than the value of the observed limiting current of Fig. 3 b (1 M acetone).

ii) The limiting current and the acetone concentration are not in a

proportional relation at high concentration (Fig. 4), while their reciprocal values are in a linear relation as shown in Fig. 8.

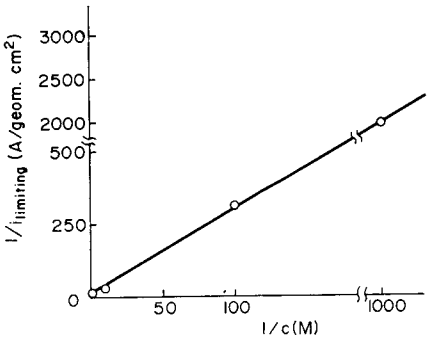


**Fig. 8.** Plot between the reciprocal of the limiting current and that of the acetone concentration (platinized-Pt, He-saturated 6N $H_2SO_4$).

The above mentioned nature leads us to conclude that the limiting current is not due to the diffusion of the reactant from the solution to the electrode surface. As seen from Fig. 4, the limiting current is independent of the proton concentration. Existence of the linear relation in Fig. 8 clearly shows that the adsorption step of acetone is in equilibrium according to the LANGMUIR isotherm and that the limiting current is proportional to the concentration of the adsorbed acetone on the surface.

**4. Mechanistic consideration of the acetone electroreduction.**

Rate of an elementary reaction has been expressed by HORIUTI[14] as

$$v = \frac{kT}{\nu h} \frac{p^*}{\prod_i p^{\delta i}}, \qquad (5)$$

where $p^*$ and $p^{\delta i}$ are the Boltzmann factor of the chemical potential of the critical complex $*$ and reactant $\delta_i$, $\nu$ the stoichiometric number of the elementary reaction, and other symbols are of usual meanings. When $\delta_i$ is the adsorbed species on a catalyst, we have further the following relation,[14]

$$p^{\delta i} = \frac{\theta_{\sigma^{\delta i}}(0)}{\theta_{\sigma^{\delta i}}(\delta_i)} q^{\delta i}, \qquad (6)$$

where $\sigma^{\delta i}$ represents the adsorption site for $\delta_i$, $\theta_{\sigma^{\delta i}}(0)$ and $\theta_{\sigma^{\delta i}}(\delta_i)$ are the probability that $\sigma^{\delta i}$ is vacant or occupied by $\delta_i$, and $q^{\delta i}$ is the Boltzmann factor of the reversible work required to bring $\delta_i$ from its standard state to the vacant $\sigma^{\delta i}$. $\theta_{\sigma^{\delta i}}(\delta_i)$ is given by the statistical thermodynamics[14] as

$$\theta_{\sigma^{\delta i}}(\delta_i) \equiv \frac{QC_{\sigma^{\delta i}}(\delta_i)}{QC},$$

$$= \frac{QC_{\sigma^{\delta i}}(\delta_i)}{QC_{\sigma^{\delta i}}(0)+QC_{\sigma^{\delta i}}(\delta_1)+QC_{\sigma^{\delta i}}(\delta_2)+\cdots}, \qquad (7)$$

where $C$ represents the whole system including an electrode, solution and gas phase, $C_{\sigma^{\delta i}}(\delta_i)$ the system where a single site of interest $\sigma^{\delta i}$ on the electrode

surface is occupied by $\delta_i$, $QC$ and $QC_{\sigma^{\delta_i}}(\delta_i)$ represent their partition functions, respectively. $QC$ is expressed by the total sum of the partition functions relevant to all possible states of the system that the adsorption site of interest is vacant and occupied by adsorbates, $\delta_1$, $\delta_2 \cdots$ $\delta_3 \cdots$. The above three fundamental equations are now applied to the present case.

*4-1). Mechanism based on the crystal plane model.*

In the potential region where the TAFEL line holds, the slope is 30 mV and the reaction order with respect to the proton is two. Hence, we first assume the following reaction scheme where elementary reaction (11) is the rate-determining step.

$$H^+ + e^- \rightleftharpoons H(a) \tag{8}$$

$$A(s) \rightleftharpoons A(a) \tag{9}$$

$$A(a) + H(a) \rightleftharpoons AH(a) \tag{10}$$

$$AH(a) + H(a) \not\rightarrow AH_2(a) \longrightarrow \cdots\cdots \longrightarrow \text{Products}, \tag{11}$$

where A stands for acetone, (s) and (a) represent dissolved state in solution and adsorbed state, respectively.

Rate of the elementary reaction (11) is expressed from Eqs. (5) and (6) as

$$i = 2F \frac{kT}{hN_A} \frac{q^*}{q^{AH(a)} q^{H(a)}} \cdot \frac{\theta_{\sigma^*}(0)}{\theta_{\sigma^*}(*)} \frac{\theta_{\sigma^{AH}}(AH)\,\theta_{\sigma^H}(H)}{\theta_{\sigma^{AH}}(0)\,\theta_{\sigma^H}(0)}, \tag{12}$$

where the rate is expressed in current. In further developement of Eq. (12), we assume that the adsorption site is common among the adsorbates of AH(a), A(a) and H(a), $AH_2$(a), *etc.*, *i.e.*, $\sigma^{AH} = \sigma^A = \sigma^H \equiv \sigma$, and that a pair of the adjacent sites forms $\sigma^*$. Namely, we develop Eq. (12) on the basis of the crystal plane model for the surface reaction. In this case,

$$\theta_{\sigma^*}(0) = \{\theta_\sigma(0)\}^2. \tag{13}$$

We, next, formulate $\theta_\sigma$(AH) and $\theta_\sigma$(H) as functions of reactant activities, $a_A$, $a_{H^+}$, and the hydrogen overvoltage $\eta$. Since the adsorption site is assumed to accommodate one of the adsorbates, H(a), A(a) and AH(a), $\theta_H = (=\theta_\sigma(H))$ and $\theta_{AH}(=\theta_\sigma(AH))$ are given from Eq. (7) as*)

$$\theta_H = QC_\sigma(H)/\{QC_\sigma(0) + QC_\sigma(AH) + QC_\sigma(A) + QC_\sigma(H)\} \tag{14}$$

*) We assume that the possibility of the site $\sigma$ to be occupied by any other reaction intermediates after the rate-determining step is negligible. Even if not, the possibility will give a constant contribution in Eq. (14) since these intermediates are in equilibrium with products. Hence, the essential features of $\theta_H$ and $\theta_{AH}$ variations with respect to the potential and acetone concentration change will remain the same.

$$\theta_{AH} = QC_\sigma(AH)/\{QC_\sigma(0)+QC_\sigma(H)+QC_\sigma(A)+QC_\sigma(AH)\}. \quad (15)$$

From Eqs. (14), (15) and the relation,

$$\frac{QC_\sigma(\delta)}{QC_\sigma(0)} = \frac{QC_\sigma(\delta)/QC}{QC_\sigma(0)/QC} = \frac{\theta_\sigma(\delta)}{\theta_\sigma(0)} = \frac{q^\delta}{p^\delta}, \quad (16)$$

one obtains,

$$\theta_H \theta_{AH} = \frac{(q^H/p^H)\cdot(q^{AH}/p^{AH})}{\left(1+\frac{q^H}{p^H}+\frac{q^A}{p^A}+\frac{q^{AH}}{p^{AH}}\right)^2}. \quad (17)$$

As the elementary reactions (8), (9) and (10) are in equilibrium, the following equations are derived by equating the chemical potential of the reactants to that of products of the respective elementary reactions.

$$\frac{q^H}{p^H} = K^H a_{H^+} \exp\left(-\frac{F\eta}{RT}\right) \quad (18)$$

$$\frac{q^A}{p^A} = K^A a_A \quad (19)$$

$$\frac{q^{AH}}{p^{AH}} = \frac{q^{AH}}{p^A \cdot p^H} = K^{AH} a_A a_{H^+} \exp\left(-\frac{F\eta}{RT}\right), \quad (20)$$

where the chemical potential of electron is given by $\mu(e^-)=\text{const}-F\eta$, and $K^\delta$'s are constants provided no mutual interactions among adsorbates. Eq. (17) is rewritten by using the above three equations as,

$$\theta_H \theta_{AH} = \frac{K^H K^{AH} a_A a_{H^+}^2 \exp(-2F\eta/RT)}{\left\{1+K^H a_{H^+}\exp\left(-\frac{F\eta}{RT}\right)+K^A a_A + K^{AH} a_H a_{H^+}\exp\left(-\frac{F\eta}{RT}\right)\right\}^2}. \quad (21)$$

When both $\theta_H$ and $\theta_{AH}$ are negligibly small, that is, when overvoltage is positive enough, Eq. (21) reduces to;

$$\theta_H \theta_{AH} \longrightarrow \frac{K^H K^{AH} a_A [a_{H^+}]^2 \exp(-2F\eta/RT)}{[1+K^A a_A]^2}. \quad (22)$$

Introduction of Eqs. (13) and (22) to Eq. (12) gives the reaction order of 2 with respect to $a_{H^+}$ and the TAFEL slope of $2.3\,RT/F$, which are in agreement with the experimental results. However, the value of $\theta_H \theta_{AH}$ and hence, the current is expected to first increase with the increase of $a_A$ and then decrease *via* a maximum as seen from Eq. (21) ($a_A \rightarrow$large enough), which is not the case.

When the cathodic polarization is large enough ($\eta \ll 0$), Eq. (21) becomes

$$\theta_H \theta_{AH} \longrightarrow \frac{K^H K^{AH} a_A}{[K^H + K^{AH} a_A]^2} . \tag{23}$$

Eq. (23) predicts a limiting current the value of which, however, again decreases *via* a maximum with the increase of $a_A$. Such a dependence of the current on the acetone concentration conflicts with the experimental results in the whole potential range studied. Therefore, it is concluded that the reaction scheme from (8) to (11) cannot explain the experimental results.

*4-2). Mechanism based on the "active site" model.*

Next, we assume the following reaction scheme where the elementary reaction (25) is the rate-determining step,

$$H^+ + e^- \rightleftarrows H(a) \tag{8}$$

$$A(s) \rightleftarrows A(a) \tag{9}$$

$$A(a) \rightleftarrows A'(a) \tag{24}$$

$$A'(a) + 2H(a) \not\rightarrow AH_2(a) \longrightarrow \cdots \longrightarrow \text{Products.} \tag{25}$$

In this scheme, the adsorption sites for acetone and hydrogen are assumed to locate in different facets and the adsorbed acetone molecule diffuses to the boundary site $\sigma^{A'}$ between the facets, at which they react. Adsorption site of the critical complex now consists of a pair of the adjacent $\sigma^H$ and $\sigma^{A'}$.

(i). Rate expression

The rate of the elementary reaction (25) is formulated from Eqs. (5), (6) and the relation $\theta_{\sigma^*}(0) = \theta_{\sigma^{A'}}(0) \cdot \{\theta_{\sigma^H}(0)\}^2$, as

$$i = 2F \frac{KT}{hN_A} \frac{q^*}{q^{A'(a)}[q^{H(a)}]^2} \cdot \frac{\theta_{A'} \cdot \theta_H^2}{\theta_{\sigma^*}(*)} \tag{26}$$

$\theta_{A'}$, $\theta_H$ and $\theta_A$ (abbreviated forms of $\theta_{\sigma^{A'}}(A)$, $\theta_{\sigma^H}(H)$ and $\theta_{\sigma^A}(A)$) are given as

$$\theta_H = \frac{q^H/p^H}{1 + q^H/p^H} \tag{27}$$

$$\theta_A = \frac{q^A/p^A}{1 + q^A/p^A} \tag{28}$$

$$\theta_{A'} = \frac{q^{A'}/p^{A'}}{1 + q^{A'}/p^{A'}} . \tag{29}$$

These equations are derived by a similar procedure as that for obtaining

Eq. (17) by excluding the possibility that $\sigma^{\delta}$ is occupied by any other adsorbates. Equilibrium conditions for the elementary reactions (8), (9) and (24) give Eqs. (18), (19) and the following equation,

$$\frac{q^{A'}}{p^{A'}} = K^{A}K^{A'}a_{A}$$

and hence from Eqs. (27), (28) and (29) we have finally,

$$\theta_{H} = \frac{K^{H}a_{H^+}\exp(-F\eta/RT)}{1+K^{H}a_{H^+}\exp(-F\eta/RT)} \tag{30}$$

$$\theta_{A} = \frac{k^{A}a_{A}}{1+K^{A}a_{A}} \tag{31}$$

$$\theta_{A'} = \frac{K^{A}K^{A'}a_{A}}{1+K^{A}K^{A'}a_{A}}, \tag{32}$$

where $K^{\delta}$'s are constants.

(ii). Reaction order and the TAFEL slope

At first, when $\theta_{H}$ is porportional to $a_{H^+}$ and $e^{-F\eta/RT}$, Eq. (26) gives the reaction order of 2 with respect to $a_{H^+}$ and the TAFEL slope of 30 mV.

As also seen from Eq. (32), Eq. (26) gives a constant limiting current at high acetone concentration. According to the present results, the current in the TAFEL region reaches a constant value at acetone concentrations greater than ca. $10^{-2}$M, whereas the limiting current approaches to a constant value at *ca.* 1 M. The difference in the concentration dependence of the limiting current and the current in the TAFEL region cannot be explained by one and the same rate-determining step.

(iii). The limiting current

Rate of the elementary reaction (25) increases by the factor exp $(-2F\eta/RT)$, if all the preliminary reactions (8), (9) and (24) are in equilibrium. However, rate of the surface diffusion (24) cannot exceeds a maximum value given at a condition that the concentration of A'(a) is zero. Therefore, it will be suggested that the rate-determining step shift from the elementary reaction (25) to (24) with the increase of the negative polarization.

(iv). Adsorption of acetone on pt-Pt

We will now examine whether the behavior of I-V curve obtained by the potential sweep method is in harmony with the reaction scheme based on the "active site" model.

When the crystal plane model is assumed, the surface site can accommodate one of the three adsorbates. Thus, $\theta_{H}$ is formulated from Eqs. (14), (16), (18), (19) and (20) as

$$\theta_H = \frac{K^H a_{H^+} \exp(-F\eta/RT)}{K^H a_{H^+} \exp(-F\eta/RT) + K^{AH} a_A a_{H^+} \exp(-F\eta/RT) + K_A a_A + 1} \tag{33}$$

and at high cathodic polarization

$$\theta_H \rightarrow \frac{K^H}{K^H + K^{AH} a_A} . \tag{34}$$

From Eq. (33), $\theta_H$ is expected to decrease with the increase of the acetone concentration.

On the other hand, $\theta_H$ is expected to be independent of the acetone concentration in the case of the reaction scheme based on the "active site", model, since the adsorption sites are different for H (a) and A (a).

A platinum electrode surface is generally taken to be fully covered with hydrogen atom at RHE. Statistical mechanical calculation of the adsorption isotherm, however, shows that (111) lattice plane is only covered less than one third though the other lattice planes, (110) and (100), are fully covered.[15] Hence, it may be possible that acetone adsorbs mainly on the (111) lattice plane.

**5. Reaction mechanism of the hydrogen electrode reaction.**

As seen from Figs. 3 a and 3 b, TAFEL lines of the hydrogen electrode reaction coincide with each other on smooth-Pt and pt-Pt and are expressed by Eq. (1).

Absence of the effect of the surface roughness on the reaction rate shows that the diffusion of the hydrogen molecule evolved to the bulk of solution is the rate-determining step. Rate of the diffusion is given as

$$i = 2FDa_{H_2(s)}/\delta , \tag{35}$$

where $a_{H_2(s)}$ is the activity of the hydrogen molecule near the surface, $D$ the diffusion constant of hydrogen in water, and $\delta$ the thickness of the diffusion layer. Since the present experiment was carried out under He bubbling, the solubility of hydrogen in bulk solution $a_{H_2(b)}$ is 0. The difference of $a_{H_2(s)}$ from the value at equilibrium, $a_{H_2(s),eq}$, produces a concentration polarization, $\eta$, given by the Nernst equation as

$$\eta = \frac{RT}{2F} \ln \frac{a_{H_2(s),eq}}{a_{H_2(s)}} . \tag{36}$$

Introduction of Eq. (35) to Eq. (36) gives the following relation

$$\eta = -\frac{RT}{2F} \ln \frac{\delta}{2FDa_{H_2(s),eq}} - \frac{RT}{2F} \ln i \tag{37}$$

with the TAFEL slope of 30 mV at 25°C. The constant term of Eq. (37) does not include any parameters which reflect the nature of the electrode surface. Thus, the same value is expected both on smooth-Pt and pt-Pt.

Its value is calculated as $-0.06$ V by using $\delta$; $10^{-3}$cm, $D$; $5.2\times10^{-5}$ cm$^2$/sec,[10] and $a_{H_2(g),eq}$; solubility of hydrogen in the water, 0.0175 m$l$/m$l$.[12] The calculated value almost coincides with $-0.09$ V of Eq. (1). Presence of the bubbling effect on the TAFEL relation also supports the conclusion that the hydrogen electrode reaction is governed by the diffusion of the evolved hydrogen molecule.

**6. Behavior of the open circuit potential.**

An open circuit potential is determined by the anodic and cathodic reactions which proceed with an equal rate, *i. e.*, the ionization of the dissolved hydrogen molecules and the reduction of acetone in the present case.

The open circuit potential of *ca.* $+100$ mV observed on pt-Pt will be explained as follows. Anodic current on pt-Pt is $+2.55$ mA/cm$^2$ at potentials more positive than $+100$ mV (Table 2), whereas a cathodic current of $-2\sim-7$ mA/cm$^2$ is attained at $+100$ mV as seen from Fig. 3 b. Therefore, the open circuit potential on pt-Pt will appear around *ca.* $+100$ mV. At a small acetone concentration($\leqq10^{-3}$M), the acetone reduction becomes slow and the open circuit potential will shift in the negative direction to accelerate the acetone reduction.

In the case of smooth-Pt, the open circuit potential is found at *ca.*$+10$ mV, even at 1 M of acetone concentration. At this potential, the ionization current of the dissolved hydrogen is reported as $+0.9$ mA/cm$^2$[8] whereas the cathodic current is $-1.1\sim-1.4$ mA/cm$^2$ from Fig. 4 a. Their absolute values are almost equal with each other.

It is noticed in Fig. 1 that the open circuit potential on pt-Pt shifts gradually in the negative direction with the increase of acetone concentration above $10^{-2}$M. The shift will be due to the decrease in the viscosity of the solution with the increase of the acetone concentration. The viscosity coefficient of water is 1.005 [cp][12] and that of acetone is 0.322 [cp].[12] The decrease in the frictional force will cause the increase in the diffusion rate and hence the ionization current of the dissolved hydrogen molecule. The increase of the anodic ionization current should be compensated by the same amount of increase of the cathodic current at the open circuit. The increase of the cathodic current is only attained by the shift of the potential in the negative direction since its rate is controlled by the potential dependent surface reaction.

## References

1) L. I. ANTROPOV, Zhur. Fiz. Khim., **24**, 1428 (1950); **26**, 1688 (1952).
2) H. KITA, Nippon Kagaku Zasshi, **92**, 99 (1971).
3) K. FUJIKAWA, H. KITA and K. MIYAHARA, J. C. S. Faraday I, **69**, 481 (1973).
4) J. N. BUTLER and A. C. MAKRIDES, Trans. Faraday Soc., **60**, 938 (1964).
5) B. E. CONWAY and M. SALOMON, J. Chem. Phys., **41**, 3169 (1964).
6) O. NAGASHIMA and H. KITA, J. Res. Inst. Catalysis, Hokkaido Univ., **15**, 49 (1967).
7) H. KITA and S. ISHIKURA and A. KATAYAMA, Electrochim. Acta, **19**, 555 (1974).
8) M. NAKAMURA and H. KITA, Denki Kagaku, **10**, 41 (1973).
9) A. FRUMKIN, Trans. Faraday Soc., **36**, 117 (1940).
10) *International Critical Tables of Numerical Data, Physics, Chemistry and Technology*, Vol. **5**, 1929.
11) X. DE. HEMPTINNE and K. SCHUNCK, Ann. Soc. Sc. Bruxelles, **80**, 289 (1966); Trans. Faraday Soc., **65**, 591 (1961).
12) *Handbook of Chemistry*, Fundamental II, Chemical Society of Japan, Maruzen, Japan (1966).
13) *American Institute of Physics Handbook*, Third Edition, 2-228, McGraw Hill (1972).
14) J. HORIUTI, J. Res. Inst. Catalysis, Hokkaido Univ., **1**, 8 (1948).
15) H. KITA, J. Res. Inst. Catalysis Hokkaido Univ., **17**, 77 (1969).